

Full Paper

Second law analysis of laminar flow in a channel filled with saturated porous media: a numerical solution

Kamel Hooman¹, Arash Ejlali²

¹Mechanical Engineering Department, Persian Gulf University, Bushehr, Iran (Hooman@pgu.ac.ir)

²Fix Equipment Lead Engineer, Namavaran Delvar Engng. & Construction Company, Tehran, Iran

Received: 2 November 2005 / Accepted: 8 December 2005 / Published: 9 December 2005

Abstract

This paper investigates entropy generation due to forced convection in a porous medium sandwiched between two parallel plates one of them being subjected to a uniform heat flux and the other one insulated. Our results showed that viscous dissipation will affect the entropy generation rate at the centerline of the channel since viscous dissipation is a quadratic function of velocity [1-3]. Neglecting the Darcy dissipation term in comparison with the terms added by Al-Hadrami et al. [4], will lead to the misunderstanding that fluid friction has no effect on the entropy generation rate at the tube centerline where the velocity derivative vanishes due to symmetry. Though the term added by [4] is $O(Da)$ compared to the Darcy term one should not drop it unless the clear flow solution is sought [5-7]. Moreover, as stated by Nield [1], one should not use just the term involving velocity derivatives, as some authors have done in the past, for example [8-11]. Though in this paper the viscous dissipation effects in the energy equation are neglected, we have taken them into account when it came to the entropy generation analysis.

Keywords: Porous medium, Forced convection, Entropy generation, Viscous dissipation

Problem statement

Figure 1 shows the problem under consideration. When the flow in hydrodynamically fully developed one knows that the Brinkman flow model leads to the following momentum equation

$$\frac{d^2u}{dy^2} - s^2u + 1 = 0. \tag{1}$$

with the porous medium shape factor s being defined as $S=a/K^{1/2}$ wherein K is the permeability and a is the channel width.

Defining $\theta = k \frac{T - T_{in}}{q''a}$, the thermal energy equation in the absence of flow work, viscous dissipation, thermal dispersion and axial conduction effect is

$$\hat{u} \frac{\partial \theta}{\partial x} = Pe \frac{\partial^2 \theta}{\partial y^2}. \tag{2}$$

where \hat{u} is the normalized velocity (local velocity divided by the average velocity, i.e. $\hat{u} = u/U$), the Péclet number is $Pe = \frac{\rho c_p a U}{k}$, k is the effective thermal conductivity, ρ is the fluid density, c_p is the specific at constant pressure, and q'' is the wall heat flux. The dimensionless coordinates are $(x,y) = (\bar{x}, \bar{y})/a$ and the thermal boundary conditions are $\theta = 0$ when $x=0$, $\frac{\partial \theta}{\partial y} = -1$ at the bottom wall

and $\frac{\partial \theta}{\partial y} = 0$ at the top wall.

Another alternative is to apply the following separation procedure

$$\frac{\partial \theta}{\partial x} = \frac{\partial^2 \theta}{\partial y^2} = \lambda \tag{3}$$

The above will lead to two ordinary differential equations that one of them needs numerical integration to be solved while the other one leads to a simple exponential answer.

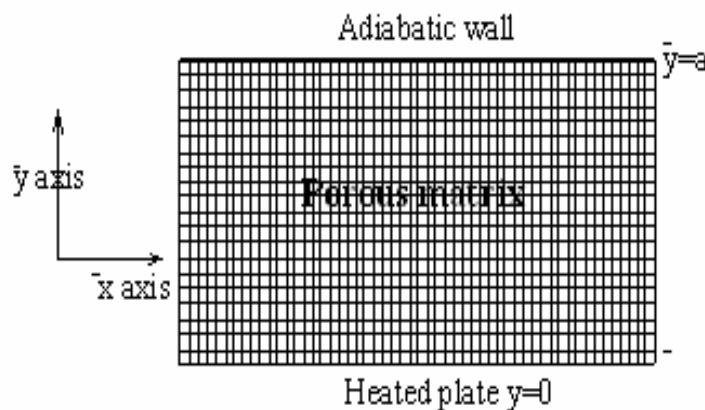


Figure 1 Definition sketch.

Numerical details

A numerical solution is presented for the momentum and the thermal energy equation, i.e. Eqns. (1-2) subjected to the aforementioned boundary conditions. To achieve this goal, we applied an implicit finite difference scheme, backward in x and central in y . Details of the method may be found in [12] and so we neglect repeating them. Length to height ratio of the channel is set at 10. A 0.05×0.005 grid system is applied and it is observed that moving from this grid to a more intense one- being 0.001×0.0001 - will change the results within less than 1%. Changing the thermal boundary condition to a constant heat flux wall, we validated our work by defining a Nusselt number $Nu = ha/(2k)$. It is observed that our predicted Nu differs from that of [3] in the fourth figure. One may recover the known analytical data for this case as reported by [3]; however, the details and exact figures are not presented in this report for the sake of brevity.

We present a first law of thermodynamics approach to verify our solution. Considering a slice of the channel with the dimensions $a \cdot dx$ and applying the first law of thermodynamics, one obtains

$$q = \rho c_p a U \frac{dT_m}{d\bar{x}}, \quad (4)$$

wherein U and T_m are mean velocity and bulk temperature. Rearranging the above equation in terms of non-dimensional parameters one finds

$$\frac{d\theta_m}{d\bar{x}} = \frac{1}{aPe}, \quad (5)$$

Since a uniform temperature is applied at the channel inlet, the solution to Eq. (5) reads

$$\theta_m = \frac{\bar{x}}{aPe}. \quad (6)$$

Our work resulted in Fig. 2. This figure may also be used for validation purpose.

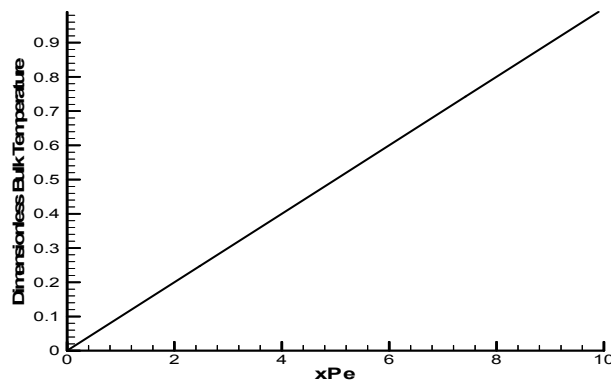


Figure 2 Dimensionless bulk temperature for $Pe=10$ (numerical results).

Results and discussion

Dimensionless temperature distribution is illustrated in Figs. 3 through 5. Showing the results, xPe is called x for short. Figures 3 and 4 are designed to illustrate the dimensionless temperature profiles in the duct cross-section for some streamwise locations. The slopes at upper and bottom walls show that

the former is adiabatic while the latter is at a constant heat flux in such a way that moving toward the upper wall both the transverse temperature gradient and the temperature itself decrease. Figure 5 shows the dimensionless temperature contours through the channel. Moving downstream, the isotherm values increase as fluid becomes heated near the bottom wall.

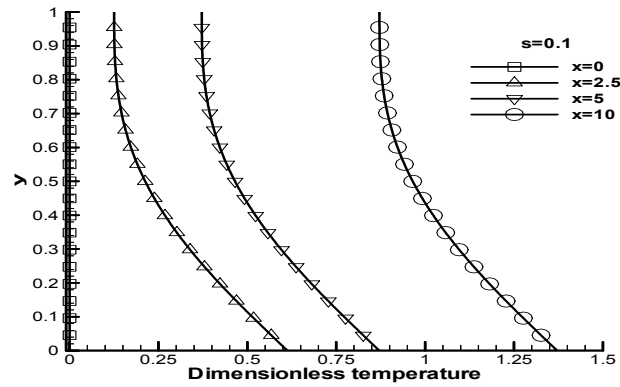


Figure 3 Dimensionless temperature distribution at different longitudinal locations ($s=0.1$)

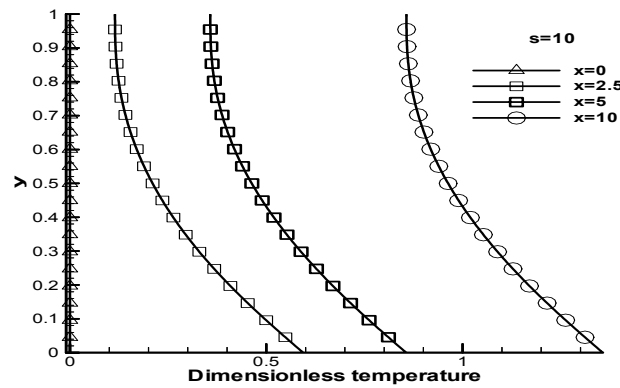


Figure 4 Dimensionless temperature distribution at different longitudinal positions ($s=10$)

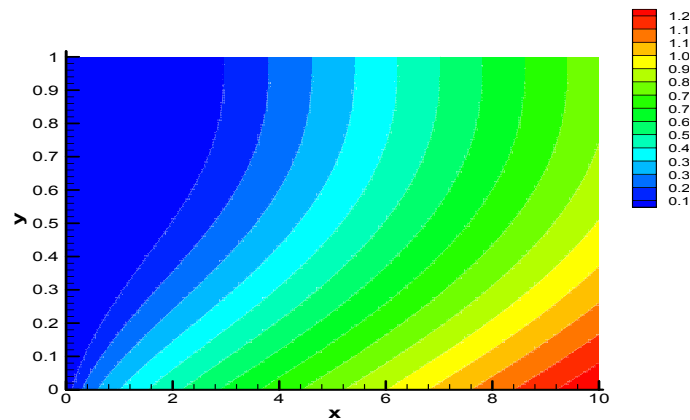


Figure 5 Dimensionless temperature contours ($s=0.1$)

Figures 6 through 10 illustrate the dimensionless entropy generation rate, Ns , for some values of s and Br while in all figures the values of Pe and Ω are fixed to 10 and 1, respectively. As a common trend in all figures one comprehends that the entropy generation rate decreases from the channel inlet to the outlet due to a fall in temperature gradients and this plunge is associated with a decrease in the heat transfer irreversibility term. As seen, for small values of s the plots of Ns experience a minimum while for large values of s one observes two local minima. For large values of s , the velocity changes in a thin region adjacent to the walls and this is accompanied by a steep temperature gradient near the bottom wall leading to a local maximum for Ns that happens near the bottom wall. Though near the upper wall the temperature gradients are small, Ns reaches a local maximum for a decrease in the temperature appearing in the denominator of Ns . Ns is defined here similar to Bejan [13], without the assumption that temperature difference in a cross-section is small, as

$$Ns = \frac{\left(\frac{\partial\theta}{\partial x}\right)^2 + \left(\frac{\partial\theta}{\partial y}\right)^2}{(\Omega + \theta)^2} + \frac{Br}{(\Omega + \theta)} \left(s^2 u^2 + \left(\frac{du}{dy}\right)^2 \right). \quad (7)$$

Some authors have dropped the denominators to define an entropy generation number but this definition may work out to be a representative of entropy generation rate only if $\frac{1}{\Omega}$, i.e. $\frac{kT_{in}}{q''a}$ is negligible, as stated by Bejan [13] and applied by some authors [14-17]. This can be mathematically interpreted as $\Omega \gg \theta$; which is not the case here.

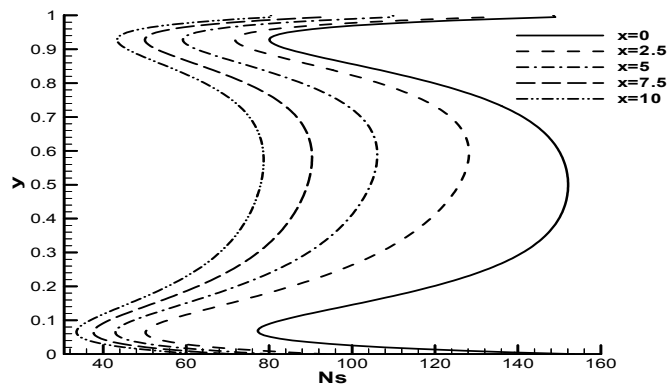


Figure 6 Ns versus y for some longitudinal locations ($s=10$ and $Br=1$).

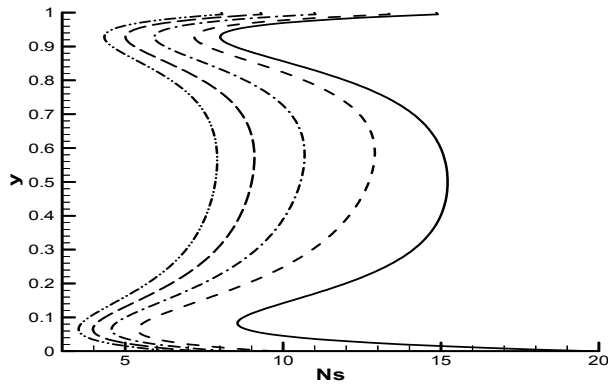


Figure 7 Ns versus y for some longitudinal locations; $s=10$, $Br=0.1$ (legends identified on Fig. 6).

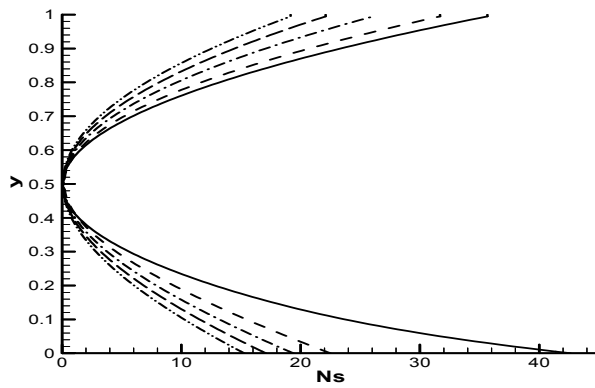


Figure 8 Ns versus y for some longitudinal locations; $s=0.1$, $Br=1$ (legends are identified on Fig. 6).

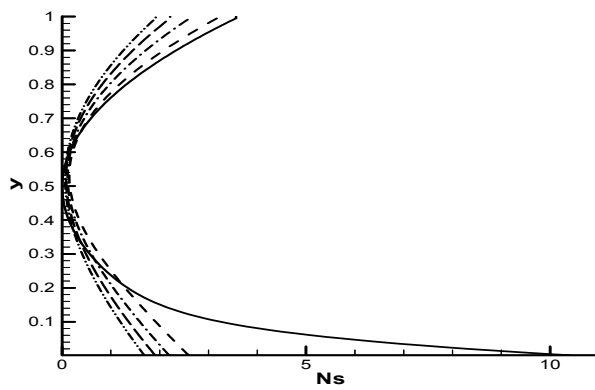


Figure 9 Ns versus y for some x with $s=0.1$ and $Br=0.1$ (legends are identified on Fig. 6).

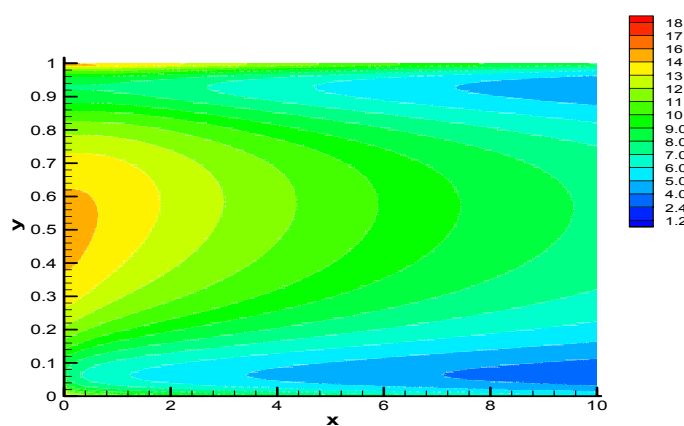


Figure 10 Ns contours through the channel ($s=10$ and $Br=0.1$).

Far from the walls, in the channel centerline regions, the velocity is distributed somehow uniformly so that the velocity gradients are small in this region. On the other hand, the velocity magnitude contributes to fluid friction irreversibility (FFI). For this reason, unlike small s cases, the entropy generation plot will not pass through one minimum in the channel centerline. Actually, when s is large Ns recovers in the channel centerline for the velocity attains its maximum in this region and this fact is much more voiced for higher values of Br . Comparing Fig. 6 with Fig. 7, one realizes that moving from $Br=0.1$ to $Br=1$ with $s=10$ stretches the Ns plot by a factor, say, approximately 8. The two minima for large s will happen near the walls and for small s the so-called minimum takes place at the centerline. However, the maximum entropy generation rate depends on the interaction between heat transfer and fluid friction irreversibility that, in turn, depends on Pe , s , Br , and Ω .

Acknowledgments: We are indebted to Professor D.A. Nield of the University of Auckland for his improving comments.

References

1. Nield, D. A., Comments on ‘A new model for viscous dissipation in porous media across a range of permeability values’ by A. K. Al-Hadhrami, L. Elliott and D. B. Ingham, *Transport Porous Media* **2004**, *55*, 253-254.
2. Bejan, A., *Convection Heat Transfer*, Wiley, 1984.
3. Nield DA, Bejan, A., *Convection in Porous Media*, 2nd Ed., Springer-Verlag, 1999.
4. Al-Hadrami, A.K., Elliott, L., Ingham, D.B., A new model for viscous dissipation in porous media across a range of permeability values, *Transport Porous Media* **2003**, *53*, 117-122.
5. Nield DA, Private communications, **2005**.
6. Nield, D.A., Resolution of a paradox involving viscous dissipation and nonlinear drag in a porous medium, *Transport Porous Media* **2000**, *41*, 349-357.

7. Nield, D.A., Modelling fluid flow in saturated porous media and at interfaces, in *Transport Phenomena in Porous Media II* (D.B. Ingham and I. Pop), Elsevier Science, Oxford, **2002**.
8. Tasnim, S.H., Mahmud, S., M.A.H. Mamun, Entropy generation in a porous channel with hydromagnetic effect, *Exergy, Int. J.* **2002**, *2*, 300-308.
9. Mahmud, S., Fraser, R.A., Flow, thermal, and entropy generation characteristics inside a porous channel with viscous dissipation, *Int. J. Thermal Sci.* **2005**, *44*, 21-32.
10. Mahmud, S., Fraser, R.A., Entropy-energy analysis of porous stack: steady state conjugate problem, *Int. J. Exergy* **2004**, *1*(3), 387-398.
11. Mahmud, S., Fraser, R.A., Mixed convection-radiation interaction in a vertical porous channel: entropy generation, *Energy* **2003**, *28*, 1557-1577.
12. Tannehill, J.C., Anderson, D.A., Pletcher, R.H., *Computational Fluid Mechanics and Heat Transfer*, 2nd Ed., Taylor & Francis, 1997.
13. Bejan, A., *Entropy generation through heat and fluid flow*, Wiley, 1982.
14. Ibanez, G., Cuevas, S., and Lopez de Haro, M., Heat transfer in asymmetric convective cooling and optimized entropy generation rate, *Rev. Mex. Fis.* **2003**, *49*(4), 338-343.
15. Hooman, K., Fully Developed Temperature Distribution in a Porous Saturated Duct of Elliptical Cross-Section, with Viscous Dissipation Effects and Entropy Generation Analysis, *Heat Transfer Research* **2005**, *36*(3), 237-245.
16. Hooman, K., Second Law Analysis of Thermally Developing Forced Convection in a Porous Medium, *Heat Transfer Research* **2005**, *36*(6), 437-447.
17. Hooman, K., Analysis of entropy generation in porous media imbedded inside elliptical passages, *Int. J. Heat Tech.*, **2005** *23*(1), to appear.